Quadrupole and octupole collectivity in the semi-magic nucleus $^{206}_{80}Hg_{126}$

L. Morrison[a,*], K. Hadyńska-Klęk[b,a], Zs. Podolyák[a], L.P. Gaffney[c,d], M. Zielińska[e], B.A. Brown[f], H. Grawe[g,1], P.D. Stevenson[a], T. Berry[a], A. Boukhari[h], M. Brunet[a], R. Canavan[a,i], R. Catherall[d], J. Cederkäll[j], S.J. Colosimo[k,l], J.G. Cubiss[m,d], H. De Witte[n], D.T. Doherty[a], Ch. Fransen[o], G. Georgiev[p,h], E. Giannopoulos[q,d], M. Górska[g], H. Hess[o], L. Kaya[o], T. Kröll[r], N. Lalović[j], B. Marsh[d], Y. Martinez Palenzuela[d,n], G. O'Neill[s,t], J. Pakarinen[q], J.P. Ramos[d,2], P. Reiter[o], J.A. Rodriguez[d], D. Rosiak[o], S. Rothe[d], M. Rudigier[a], M. Siciliano[e,u], E.C. Simpson[v], J. Snall[d,j], P. Spagnoletti[w], S. Thiel[o], N. Warr[o], F. Wenander[d], R. Zidarova[d]

[a] *Department of Physics, University of Surrey, Guildford, GU2 7XH, United Kingdom*
[b] *Heavy Ion Laboratory, University of Warsaw, Ludwika Pasteura 5A, 02-093 Warszawa, Poland*
[c] *Oliver Lodge Laboratory, University of Liverpool, Liverpool, L69 7ZE, United Kingdom*
[d] *CERN, Physics Department, 1211 Geneva 23, Switzerland*
[e] *IRFU, CEA, Université Paris-Saclay, F-91191 Gif-sur-Yvette, France*
[f] *Department of Physics and Astronomy, FRIB Laboratory, Michigan State University, East Lansing, MI 42284-1321, USA*
[g] *GSI Helmholtzzentrum für Schwerionenforschung GmbH, Planckstrasse 1, 64291 Darmstadt, Germany*
[h] *CSNSM, Univ. Paris-Sud, CNRS/IN2P3, Université Paris-Saclay, F-91405 Orsay, France*
[i] *National Physical Laboratory, Hampton Rd., Teddington, TW11 0LW, United Kingdom*
[j] *Physics Department, Lund University, Box 118, Lund SE-221 00, Sweden*
[k] *National Health Service Grampian, Aberdeen Royal Infirmary, Aberdeen, AB25 2ZN, Scotland*
[l] *School of Medicine, Medical Sciences and Nutrition, University of Aberdeen, Foresterhill Health Campus, Foresterhill Rd., Aberdeen, AB25 2ZN, Scotland*
[m] *Department of Physics, University of York, Heslington, York, YO10 5DD, United Kingdom*
[n] *KU Leuven, Instituut voor Kern-en Stralingsfysica, B-3001 Leuven, Belgium*
[o] *IKP Köln, Zülpicher Str. 77, 50937 Köln, Germany*
[p] *IJCLab, Université Paris-Saclay, F-91405 Orsay, France*
[q] *Department of Physics, University of Jyväskylä, P.O. Box 35 (YFL), Jyväskylä, FI-40014, Finland*
[r] *Technische Universität Darmstadt, Institut für Kernphysik, Schlossgartenstr. 9, 64289 Darmstadt, Germany*
[s] *Department of Physics and Astronomy, University of the Western Cape, P/B X17, Bellville, ZA-7535, South Africa*
[t] *iThemba LABS, Old Faure Road, Faure, Cape Town, 7131, South Africa*
[u] *INFN Laboratori Nazionali di Legnaro, 35020 Legnaro (Pd), Italy*
[v] *Department of Nuclear Physics, Research School of Physics, Australian National University, Canberra ACT 2601, Australia*
[w] *School of Computing, Engineering and Physical Sciences, University of the West of Scotland, Paisley PA1 2BE, United Kingdom*

Abstract

The first low-energy Coulomb-excitation measurement of the radioactive, semi-magic, two proton-hole nucleus ^{206}Hg, was performed at CERN's recently-commissioned HIE-ISOLDE facility. Two γ rays depopulating low-lying states in ^{206}Hg were observed. From the data, a reduced transition strength $B(E2; 2_1^+ \rightarrow 0_1^+) = 4.4(6)$ W.u was determined, the first such value for an $N = 126$ nucleus south of ^{208}Pb, which is found to be slightly lower than that predicted by shell-model calculations. In addition, a collective octupole state was identified at an excitation energy of 2705 keV, for which a reduced $B(E3)$ transition probability of 30^{+10}_{-13} W.u was extracted. These results are crucial for understanding both quadrupole and octupole collectivity in the vicinity of the heaviest doubly-magic nucleus ^{208}Pb, and for benchmarking a number of theoretical approaches in this key region. This is of particular importance given the paucity of data on transition strengths in this region, which could be used, in principle, to test calculations relevant to the astrophysical r-process.

Many-body quantum systems exhibit shell structures, a concept first introduced in order to explain the properties of electrons in an atom [1]. Later, the shell model was successfully used for diverse systems from atomic nuclei [2], to metallic clusters [3]. In nuclei, the doubly-magic species, with magic numbers of protons and neutrons, act as cornerstones of the nuclide chart. Recently, studies of nuclei with extreme neutron-to-proton ratios have shown that the traditional magic numbers can erode, and in the case of light nuclei, even new ones may appear [4]. In heavier systems, such as those around ^{132}Sn [5] and ^{208}Pb, shell evolution is under intense scrutiny, motivated also by their role in the nucleosynthesis of elements heavier than iron in the astrophysical rapid neutron-capture (r)-process [6].

The $^{208}Pb_{126}$ nuclide is the heaviest-known doubly-magic nucleus. Nuclei in its vicinity are special in two

*Corresponding author
Email address: l.n.morrison@surrey.ac.uk (L. Morrison)
[1] Deceased
[2] Present address: SCK CEN, Boeretang 200, 2400 Mol, Belgium

ways: (i) they exhibit strong octupole collectivity (as illustrated by the first excited state of ^{208}Pb at 2.615 MeV with spin-parity 3^-), and (ii) the information on its neutron-rich neighborhood is rather scarce, due to the limited mechanisms by which these nuclei can be populated. Experimental information on neutron-rich N∼126 nuclei is of paramount importance not only for within nuclear-structure physics, but also for implications within astrophysics. Data on transition strengths is scarce, although in principle, these could provide stringent constraints for a variety of theoretical calculations, including those predicting the properties of nuclei on the *r*-process path.

Neutron-rich nuclei around ^{208}Pb are under intense scrutiny, with pioneering experiments performed to address their ground-state properties [8–10], as well their excited states [11, 12]. Mass and charge radii measurements indicate the magicity of $N = 126$ for the mercury ($Z = 80$) isotopes [8, 10]. However, no $B(E2; 2^+ \rightarrow 0^+)$ transition strengths have been extracted for any of the $N = 126$ nuclei below ^{208}Pb. This quantity, connected to the wave functions of the involved states, often provides the first hint of the erosion of magicity by exhibiting enhanced collectivity. In this *Letter*, we present results of the first dedicated low-energy Coulomb-excitation experiment of any semi-magic nucleus 'south of' ^{208}Pb, providing insight into both quadrupole and octupole collectivity in this mass region.

To date, ^{206}Hg$_{126}$ has been populated in a broad range of experiments [9–11, 13–24]. However, so far only yrast states have been observed [25], including the 5^- and 10^+ isomers, without any hint of the expected low-energy collective 3^- level.

A radioactive beam of ^{206}Hg was produced at the HIE-ISOLDE facility at CERN using a molten lead target bombarded with 1.4 GeV protons, with an intensity of $\approx 0.6\ \mu$A. The produced mercury isotopes were laser ionised (VADLIS mode) [24], mass separated using the General Purpose Separator (GPS), and charge bred in an electron-beam ion source (REX-EBIS) [26]. ^{206}Hg^{46+} ions were post-accelerated using the newly-upgraded HIE-ISOLDE linear accelerator [27, 28], to an energy of 4.195 MeV/u, with a beam repetition rate of 300 ms (3.33 Hz). The typical ^{206}Hg beam intensity was $\sim 7.8 \times 10^5$ pps.

The accelerated beam impinged on a 2 mg/cm^2 thick target, made either of ^{94}Mo or ^{104}Pd. These well-characterized targets were chosen as Cline's safe distance criterion [38] is fulfilled for the available beam energy, ensuring a purely electromagnetic interaction between the collision partners. Following Coulomb excitation, γ rays depopulating states in both the projectile and target nuclei were detected by the 23 HPGe detectors comprising the Miniball array [29], in coincidence with recoiling particles detected in an annular Double-Sided Silicon Strip Detector (DSSSD). Both sides of the DSSSD array consisted of 4 quadrants, with the front of each divided into 16 annular rings ('strips'), and the back into a further 24 sectors, coupled into 12 pairs when read out [29, 30]. This covered a scattering angle range from 20 to 59° in the laboratory reference frame.

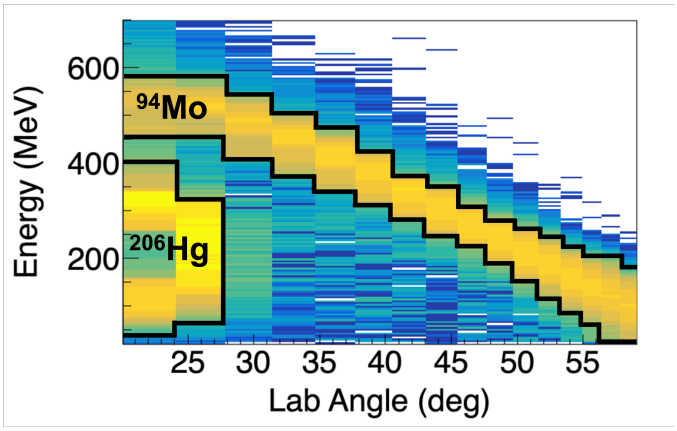

Figure 1: (Color online) Energy spectrum of the particles detected in the DSSSD as a function of the laboratory scattering angle. The regions of the ^{206}Hg projectile and recoiling ^{94}Mo target nuclei are marked. The effect of the ^{130}Xe beam contaminant was removed (for further details, see Ref. [31]).

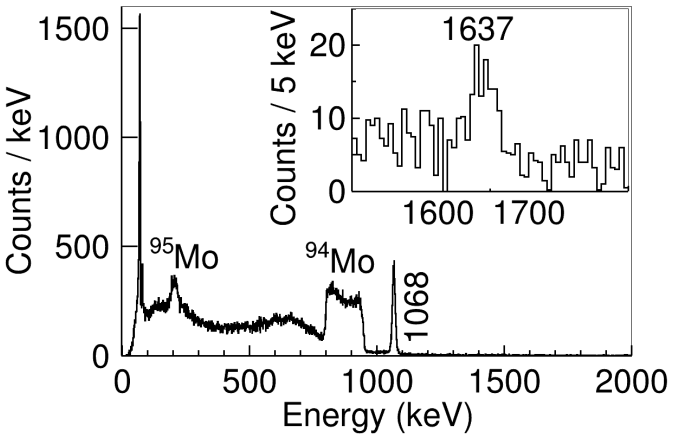

Figure 2: Background-subtracted γ-ray spectrum measured in coincidence with recoiling ^{94}Mo target-like particles registered in the DSSSD, Doppler corrected for ^{206}Hg. The effect of the ^{130}Xe contaminant was subtracted. The inset shows a zoomed-in portion of the spectrum.

During the experiment, the stable ^{130}Xe^{29+} nucleus was identified as a beam contaminant with an intensity of $\sim 3 \times 10^5$ pps. Therefore, additional runs were performed without the presence of ^{206}Hg in the beam, thus allowing the effect of the ^{130}Xe contaminant on the main ^{206}Hg data to be accounted for, as described in Ref. [31]. A separate Coulomb-excitation analysis of ^{130}Xe was presented in a dedicated publication [32], where details such as data sorting, and time conditions applied during the current ^{206}Hg analysis, were provided in detail. The beam composition was checked using an ionisation chamber, and no other contaminant was found. The reaction-kinematics plot obtained for the ^{94}Mo target measurement using the DSSSD detector, after the removal of the ^{130}Xe beam contaminant, is shown in Figure 1. The γ-ray spectrum collected in coincidence with ^{94}Mo target nuclei, Doppler corrected

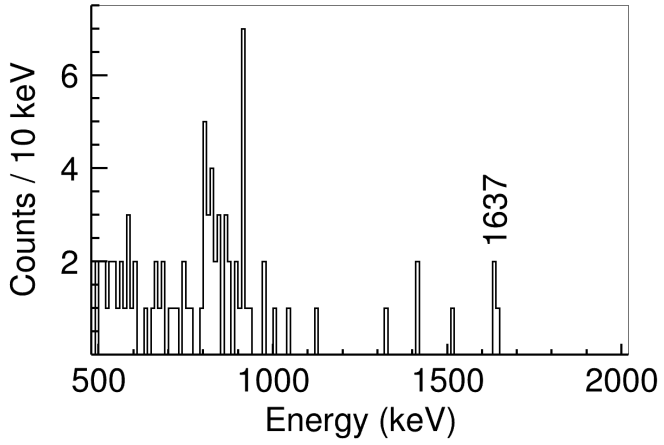

Figure 3: Coincidence γ-ray spectrum gated on the 1068 keV transition of ^{206}Hg. The γ ray visible at ~ 1.6 MeV has three counts, in line with expectations for a coincident transition. The counts below 1 MeV are mainly from cross-coincidences with the ^{94}Mo target.

for the velocity of ^{206}Hg (and cleaned of the ^{130}Xe contaminant), is shown in Figure 2.

The previously-known $2_1^+ \rightarrow 0_1^+$ transition at 1068 keV in ^{206}Hg is clearly identified in the collected γ-ray spectrum [25]. Furthermore, a low-intensity peak at 1637(2) keV is observed. The structures at around 200 and 850 keV correspond to Doppler-broadened target excitations: the $2_1^+ \rightarrow 0_1^+$ 871 keV transition in ^{94}Mo [33], and the $3/2_1^+ \rightarrow 5/2_1^+$ 204 keV transition in ^{95}Mo [34]. The ^{95}Mo component of the predominantly ^{94}Mo target was determined to be 5(1)%. This agrees with the values obtained from previous experiments using the same target: 4.4(11)% [35] and 5(2)% [36]. The 1068 keV transition in ^{206}Hg is in prompt coincidence with the newly-identified 1637 keV γ-ray transition (see Figure 3). This defines a new excited state at an excitation energy of 2705(2) keV. No γ ray was observed at 2705 keV.

In order to determine the electromagnetic properties of ^{206}Hg, data analysis was performed using the least-squares search codes `GOSIA` [37] and `GOSIA2` [38]. Since the lifetime of the 2_1^+ state is unknown, an iterative procedure with alternating use of the codes `GOSIA` and `GOSIA2` was employed to determine reduced matrix elements in ^{206}Hg, with normalization to target excitation. This method is discussed in detail in Refs. [35, 39]. Due to the proximity of the 2_1^+ state in both ^{104}Pd and the ^{130}Xe contaminant, normalization to the ^{94}Mo target was used. The first step of data analysis focused solely on the correlation between the $B(E2; 2_1^+ \rightarrow 0_1^+)$ and spectroscopic quadrupole moment of the 2_1^+ state in ^{206}Hg. Statistics in the $2_1^+ \rightarrow 0_1^+$ transition were subdivided into 7 angular ranges, and the total spectrum was introduced as an eighth data set. The $B(E2; 2_1^+ \rightarrow 0_1^+)$ value for the ^{206}Hg beam could then be extracted from the two-dimensional χ^2 surface map, calculated using the `GOSIA2` program together with a specially-developed χ^2 surface code [40], by performing a minimization with respect to the $\langle 2_1^+ \| E2 \| 0_1^+ \rangle$ and $\langle 2_1^+ \| E2 \| 2_1^+ \rangle$ matrix elements. The value of the $\langle 2_1^+ \| E2 \| 0_1^+ \rangle$ matrix element was later used as a normalization parameter in the second step of data analysis performed using the standard `GOSIA` code. Here, a second excitation was introduced at a level energy of 2705 keV, together with the corresponding 1637 keV transition depopulating the newly observed state. In this step, data from the $2_1^+ \rightarrow 0_1^+$ transition, collected during runs with the ^{104}Pd-only target, were used. The results of this stage were taken further in step 3 with the use of the `GOSIA2` code, during which the first step is essentially repeated, this time with the inclusion of the extra state, as well as the 1637 keV transition, collected for the total spectrum using the ^{94}Mo target. Further steps of the analysis involved repetition of the second and third steps, re-running this iterative procedure until the solution stabilized.

The biggest challenge of the current study was related to the unknown low-spin level scheme of ^{206}Hg. The analysis was therefore performed assuming different possible scenarios, with various spin-parity assignments of the newly-established 2705 keV state. The use of inverse kinematics with particle detection at forward laboratory angles does not favour a population of states in a multiple Coulomb-excitation process. Instead, one or two-step excitations should be considered. Furthermore, theory indicates that excited states can be populated with notable yields only via $E2$ and $E3$ interactions [41]. Several different spin assignments were considered for the 2705 keV level (see details in [42]). The 2^+ assumption returns $B(E2; 2_2^+ \rightarrow 2_1^+) = 71^{+9}_{-19}$ W.u., the 0^+ results in $B(E2; 0_2^+ \rightarrow 2_1^+) = 3460^{+387}_{-581}$ W.u., and the 4^+ assumption returns $B(E2; 4_1^+ \rightarrow 2_1^+) = 34^{+5}_{-5}$ W.u. These values are all too large for a nucleus with only two valence particles. The only realistic solution is that the 2705 keV state is populated directly via an $E3$ interaction. This results in experimental transition strength values of $B(E2; 2_1^+ \rightarrow 0_1^+) = 4.4(6)$ W.u. and $B(E3; (3_1^-) \rightarrow 0_1^+) = 30^{+10}_{-13}$ W.u., and a spectroscopic quadrupole moment of $Q_s(2_1^+) = 0.0(6)$ eb.

In order to gain a quantitative understanding of the low-spin structure of ^{206}Hg, shell-model calculations have been performed. Due to the role of octupole collectivity in the vicinity of ^{208}Pb, a large model space covering two full shells for both protons ($Z = 50 - 126$) and neutrons ($N = 82 - 184$) [43], had to be considered. Such a selection results in 24 orbitals in total, with eight $\Delta j = \Delta l = 3$ pairs across the $Z = 82$ and $N = 126$ gaps. The cross-shell two-body matrix elements (TBMEs) are based on the M3Y interaction [44], and neutron-proton, particle-particle and hole-hole TBMEs using the Kuo-Herling interaction [45] as modified in Ref. [46]. Relative to the closed-shell configuration of ^{208}Pb, the configurations were truncated to two-hole ($2h$) π^{-2} ($t = 0$), or one-particle three-hole ($1p - 3h$) $\pi^1\pi^{-3}$ and $\nu^1\pi^{-2}\nu^{-1}$ ($t = 1$). The mixing between the $t = 0$ and $t = 1$ states was not taken into account. With such a truncation, the single-particle and single-hole energies are given by experimental separation energies for

$A = 207$ and $A = 209$ relative to ^{208}Pb, as shown in Figure 1 of [46]. This parametrization describes well the known level schemes of the $N = 126$ ^{206}Hg, ^{205}Au, ^{204}Pt, and ^{203}Ir nuclei [18, 19, 47, 48].

In order to describe the $B(E2; 2_1^+ \rightarrow 0_1^+)$ transition strength, a standard effective proton charge of $e_\pi = 1.5e$ was employed, similarly as in [18, 19]. The experimental $B(E2; 10^+ \rightarrow 8^+)$ transition strength from the 10^+ isomer, as well as the measured quadrupole moment of the 5^- isomeric state [15, 52], are reproduced (see Table 1). Since both the yrast 8^+ and 10^+ states are of pure $\pi h_{11/2}^{-2}$ character, the agreement of $B(E2; 10^+ \rightarrow 8^+)$ is essential, and justifies the used effective charge. The theoretical spectroscopic quadrupole moment of $Q_s(2_1^+) = 0.41$ eb is also in agreement with the experimental 0.0(6) eb value. However, the measured $B(E2; 2_1^+ \rightarrow 0_1^+) = 4.4(6)$ W.u. is slightly lower than its theoretical counterpart at 5.42 W.u. (Note that a different, recent, shell-model calculation, leads to the same conclusion [49]).

The $B(E2)$ value obtained for the ^{206}Hg nucleus fits well into the systematics of the mercury and lead isotopes presented in Figure 4. The $B(E2)$ values decrease along the mercury isotopic chain towards the $N = 126$ shell closure as collectivity decreases. The lowest $B(E2)$ strength is, therefore, observed in the semi-magic ^{206}Hg nucleus. Here, the measured $B(E2; 2_1^+ \rightarrow 0_1^+)$ value is larger than those observed in ^{206}Pb$_{124}$ and ^{210}Pb$_{128}$ nuclei with two valence neutrons around the ^{208}Pb core, reflecting the proton character of the 2^+ excitation. In ^{206}Hg, the dominant configurations for the ground and 2_1^+ states are $\pi s_{1/2}^{-2}$ and $\pi s_{1/2}^{-1} d_{3/2}^{-1}$, respectively. However, there are sizeable ($> 10\%$) other contributions predicted in both cases ($d_{3/2}^{-2}$ in the 0^+, and $d_{3/2}^{-2}$ and $s_{1/2}^{-1} d_{5/2}^{-1}$ in the 2^+). The slightly-higher theoretical $B(E2)$ value could be related to an imperfect description of the mixing between these states. Furthermore (as shown in Figure 4), the shell model predicts slightly higher $B(E2)$ values than the experimental ones also for ^{204}Hg and ^{202}Hg, whilst for ^{204,206}Pb nuclei, there is good agreement (the standard $e_\nu = 0.85e$ and $e_\pi = 1.5e$ effective charges were used [19, 49]). This also suggests that proton wave functions are not well reproduced in the mercury isotopes. Note that the $B(E2; 2^+ \rightarrow 0^+)$ value in the two-proton-particle nucleus ^{210}Po is under scrutiny as the two performed measurements are in disagreement [56, 66], and both experimental values are much lower than expected from the seniority scheme and shell model calculations [56]. The more-recent value is still a factor of 2 lower than the shell-model prediction. This discrepancy was tentatively connected to the neglecting of ^{208}Pb particle-hole excitations in the shell model, which enter most sensitively in the 2^+ states [68]. However, our calculations for ^{206}Hg suggest that the inclusion of such proton and neutron excitations actually increases the $B(E2)$ value, thus increasing the discrepancy.

The energy of the (3^-) state predicted using SM calculations for ^{206}Hg is 2657 keV, slightly lower than the newly-found experimental value of 2705 keV. The tendency of underestimating the energy of the 3^- levels is an intrinsic feature of this type of calculation, as noted for ^{208}Pb [57, 58] and all other single-particle/hole nuclei in its vicinity [57–59]. The origin of such a discrepancy is related to the truncation of multiple core excitations, qualitatively explained in [59]. The excitation energy of the octupole phonon state is similar to those observed in lighter mercury and lead isotopes with $N \leq 126$ [61]. The $B(E3; (3_1^-) \rightarrow 0_1^+) = 28$ W.u. transition strength in the ^{206}Hg isotope was calculated using the effective charges of $e_\pi = 1.35e$ and $e_\nu = 0.35e$. These effective charges reproduce the experimental $B(E3; 3^- \rightarrow 0^+) = 36$ W.u. [51] for the doubly-magic ^{208}Pb. The lower theoretical $B(E3; (3^-) \rightarrow 0^+)$ value in the ^{206}Hg nucleus compared to ^{208}Pb, as well as the generally-lower values in the mercury isotopes compared to the lead chain (see Figure 4), could be attributed to a significant contribution of the $\pi s_{1/2}^{-1} - f_{7/2}$ excitation to the octupole phonon [60]. Whilst the single-particle structure of the 3^- state is similar in both the mercury and lead isotopic chains, the lack of $\pi s_{1/2}$ protons in the ground state of the mercury isotopes reduces the overlap between these two levels.

Table 1: Comparison of the relevant experimental energies and electromagnetic properties with theoretical values based on the shell model (SM) and time-dependent Hartree-Fock (TDHF) calculations in ^{206}Hg. For details see the text.

Observable	Exp.	SM	TDHF
$E(2_1^+)$ (keV)	1068	1068	-
$B(E2; 2_1^+ \rightarrow 0_1^+)$ (W.u.)	4.4(6)	5.42	-
$E(3_1^-)$ (keV)	2705(2)	2657	2990
$B(E3)$ (W.u.)	30^{+10}_{-13}	28	26
$Q_s(2_1^+)$ (eb)	0.0(6)	0.41	-
$B(E2; 10^+ \rightarrow 8^+)$ (W.u.)	0.84(7)[a]	0.87	-
$Q_s(5^-)$ (eb)	0.74(15)[b]	0.57	-

[a] Determined using the isomeric lifetime of $T_{1/2} = 107(6)$ ns (weighted average value from [17, 19, 22]), total branching ratio 0.76(2) from [17] and ICC= 5.5(3) [67].
[b] Value from the [52] compilation, based on the measurement of [15].

Octupole collectivity in ^{206}Hg, as well as in the neighbouring ^{208}Pb and ^{204}Hg nuclei, was also addressed via Time-Dependent Hartree-Fock (TDHF) theory. Density functional calculations have been performed using static and time-dependent calculations for the ground and octupole states respectively. The SkX interaction was used [62] with a volume delta interaction (see [63] for details). The time-dependent state was initialised with an octupole boost of the form $\exp(ikr^3 Y_{30})$ acting on the spherical ground state, and the resulting time-dependent octupole response analyzed with standard linear response theory [64], to give strength functions from which the energy centroids and $B(E3)$ transition strengths are extracted. This procedure was previously applied to giant dipole resonances [64, 65], but never for a surface vibration. The

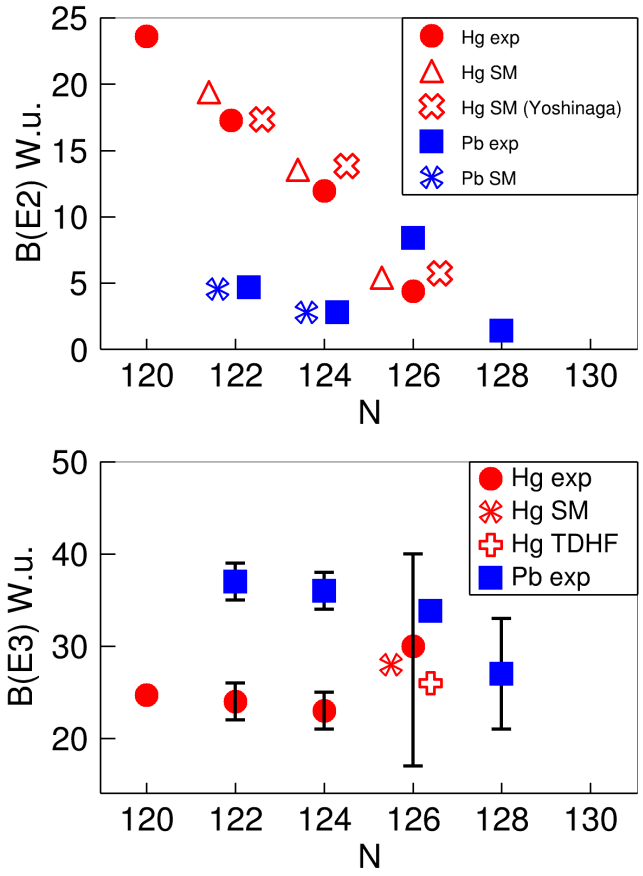

Figure 4: (Color online) Systematics of the $B(E2; 2^+ \rightarrow 0^+)$ and collective $B(E3; 3^- \rightarrow 0^+)$ reduced transition strengths for the Hg and Pb isotopes around $N = 126$ [50–55]. The displayed theoretical values are from present shell model calculations and those of Yoshinaga et al. [49]. Note that for visibility reasons, some data points are slightly shifted around the integer N values, and error bars are not indicated when they are smaller than the symbols.

calculated 3^- energies are in agreement with experimental values for ^{206}Hg ($E_{\mathrm{exp}} = 2705$ keV, $E_{\mathrm{TDHF}} = 2990$ keV), as well as for the neighbouring ^{204}Hg ($E_{\mathrm{exp}} = 2675$ keV, $E_{\mathrm{TDHF}} = 3059$ keV), and ^{208}Pb ($E_{\mathrm{exp}} = 2615$ keV, $E_{\mathrm{TDHF}} = 2602$ keV). In ^{206}Hg and ^{206}Pb, the theoretical 3^- energies are overestimated, which is attributed to the mixing with non-collective 3^- states, something not accounted for in TDHF. The $B(E3)$ transition strengths (shown on Figure 4) are in good agreement with both experimental and shell-model values. The experimental results obtained in the present work are compared with theoretical ones, obtained from both shell model and TDHF calucations, in Table 1.

In summary, the radioactive two-proton hole nucleus ^{206}Hg was Coulomb excited at safe energies at HIE-ISOLDE, yielding a $B(E2; 2^+ \rightarrow 0^+)$ value for a neutron-rich $N = 126$ nucleus for the first time. The $B(E2; 2_1^+ \rightarrow 0_1^+)$ transition strength is lower than those in the lighter Hg isotopes. It is reasonably well described by shell-model calculations considering only valence protons below $Z = 82$, supporting the closed neutron-shell character of ^{206}Hg. The small discrepancy with theory is attributed to the imperfect description of mixing with other states within the valence space, and does not imply proton-hole excitations. Information on the wave function of an individual state provided by the experiment constitutes a stringent test of nuclear theories, and could be used to restrain models employed to predict the nuclear properties of the r-process path $N = 126$ nuclei. Furthermore, the collective (3^-) state was identified close in energy, and with similar collective properties, to those found in the doubly-magic ^{208}Pb. The present results open up the prospect of studying the evolution of both quadrupole and octupole collectivity in the $N \geq 126$, $Z < 82$ region, and a means of benchmarking theoretical calculations in this important region.

The authors thank the HIE-ISOLDE accelerator division for the delivery of the beam, and all members of the Miniball collaboration. The research leading to these results has received funding from the European Union's Horizon 2020 research and innovation programme under grant agreement no. 654002 + 665779 CERN (COFUND). Support from the Science and Technology Facilities Council (UK) through grants ST/P005314/1, ST/L005743/1, ST/R004056/1, ST/J000051/1, and ST/P003885/1, the German BMBF under contracts 05P18PKCIA, 05P18RDCIA, and 'Verbundprojekt' 05P2018, and NSF (USA) grant PHY-2110365, are acknowledged. This work made use of resources at the DiRAC DiAL system at the University of Leicester, UK, (funded by the UK BEIS via STFC Capital Grants No. ST/K000373/1 and No. ST/R002363/1 and STFC DiRAC Operations Grant No. ST/R001014/1).

References

[1] N. Bohr, Phil. Mag. S. 6 **26**, 1 (1913).
[2] M. Goeppert-Mayer, Phys. Rev. **74**, 235 (1948).
[3] O. Echt, K. Sattler, E. Recknagel, Phys, Rev. Lett. **47**, 1121 (1981).
[4] T. Otsuka, A. Gade, O. Sorlin, T. Suzuki, Y. Utsuno, Rev. Mod. Phys. **92**, 015002 (2020).
[5] D. Rosiak, M. Seidlitz, P. Reiter, H. Naïdja, Y. Tsunoda, T. Togashi *et al.*, Phys. Rev. Lett. **121**, 252501 (2018).
[6] H. Grawe, K. Langanke, G. Martínez-Pinedo, Rep. Prog. Phys. **70**, 1525 (2007).
[7] J. J. Cowan, C. Sneden, J. E. Lawler, A. Aprahamian, M. Wiescher, K. Langanke, G. Martínez-Pinedo, F-K. Thielemann, Rev. Mod. Phys. **93**, 015002 (2021).
[8] L. Chen, Yu. A. Litvinov, W. R. Plaß, K. Beckert, P. Beller, F. Bosch *et al.*, Phys. Rev. Lett. **102**, 122503 (2009).
[9] R. Caballero-Folch *et al.*, Phys. Rev. Lett **117**, 012501 (2016).
[10] T. Day Goodacre, A. V. Afanasjev, A. E. Barzakh, B. A. Marsh, S. Sels, P. Ring *et al.*, Phys. Rev. Lett. **126**, 032502 (2021).
[11] T.L. Tang, B. P. Kay, C. R. Hoffman, J. P. Schiffer, D. K. Sharp, L. P. Gaffney *et al.*, Phys. Rev. Lett. **124**, 062502 (2020).
[12] R.J. Carroll *et al.*, Phys. Rev.Lett. **125**, 192501 (2020).
[13] P. Kauranen, Ann. Acad. Sci. Fennicae, Ser. A VI, No.96 (1962)
[14] J. A. Becker, J. B. Carlson, R. G. Lanier, K. H. Maier, L. G. Mann, G. L. Struble *et al.*, Phys. Rev. C **26**, 914 (1982)
[15] K. H. Maier, M. Menningen, L. E. Ussery, T. W. Nail, R. K. Sheline, J. A. Becker *et al.*, Phys. Rev. C **30**, 1702 (1984)
[16] W. R. Hering *et al.*, Phys. Rev. C **14**, 1451 (1976)
[17] B. Fornal, R. Broda, K. H. Maier, J. Wrzesiński, G. J. Lane, M. Cromaz *et al.*, Phys. Rev. Lett. **87** 212501 (2001)
[18] S.J. Steer *et al.*, Phys.Rev. C **78**, 061302(R) (2008).

[19] S.J. Steer *et al.*, Phys. Rev. C **84**, 044313 (2011).
[20] E. C. Simpson, J. A. Tostevin, Zs. Podolyák, P. H. Regan, and S. J. Steer Phys. Rev. C **80**, 064608 (2009)
[21] M. Pfützner, P. H. Regan, P. M. Walker, M. Caamaño, J. Gerl, M. Hellström, *et al.*, Phys. Rev. C **65**, 064604 (2002)
[22] N. Al-Dahan *et al.*, Phys. Rev. C **80**, 061302(R) (2009)
[23] T. Alexander *et al.*, Acta Phys. Pol. B **46**, 601 (2015).
[24] T. Day Goodacre *et al.*, Phys. Rev. C **104**, 054322 (2021).
[25] F.G. Kondev, Nucl. Data Sheets **109**, 1527 (2008).
[26] F. Wenander, J. Instrum. **5**, C10004 (2010).
[27] M. J. G. Borge and K. Riisager, Eur. Phys. J. A **52**, 334 (2016).
[28] Y. Kadi, Y. Blumenfeld, W. V. Delsolaro, M. A. Fraser, M. Huyse, A. P. Koudou, J. A. Rodriguez, and F. Wenander, J. Phys. G **44**, 084003 (2017).
[29] N. Warr et al., Eur. Phys. J. A **49**, 1 (2013).
[30] A.N Ostrowski, S. Cherubini, T. Davinson, D. Groombridge, A.M Laird, A. Musumarra, A. Ninane, A. Di Pietro, A.C. Shotter and P.J. Woods, Nucl. Instrum. Meth. Sect. A **480**, 448 (2013).
[31] L. Morrison et al., J. of Phys.: Conf. Series **1643**, 012146 (2020).
[32] L. Morrison, K. Hadyńska-Klęk, Zs. Podolyák, D. T. Doherty, L. P. Gaffney, L. Kaya *et al.*, Phys.Rev. C **102**, 054304 (2020).
[33] D. Abriola, A. A. Sonzogni, Nucl. Data Sheets **107**, 2423 (2006)
[34] S. K. Basu, G. Mukherjee, A. A. Sonzogni, Nucl. Data Sheets **111**, 2555 (2010).
[35] M. Klintefjord, K. Hadyńska-Klęk, A. Görgen, C. Bauer, F. L. Bello Garrote, S. Bönig *et al.*, Phys. Rev. C **93**, 054303 (2016).
[36] N. Kesteloot *et al.*, Phys. Rev. C **92**, 054301 (2015).
[37] T. Czosnyka, D. Cline, and C. Y. Wu, Bull. Am. Phys.Soc. **28**, 745 (1982).
[38] D. Cline, Annu. Rev. Nucl. Part. Sci. **36**, 683, (1986).
[39] M. Zielinska *et al.*, Eur. Phys. J. A **52**, 99 (2016).
[40] L.P. Gaffney, https://github.com/lpgaff/chisqsurface
[41] J. Srebrny et al., Nucl. Phys. A **557**, 663c (1993).
[42] L. Morrison, PhD thesis, University of Surrey, UK, 2021.
[43] B. A. Brown, Phys. Rev. Lett. **85**, 5300 (2000).
[44] G. Bertsch et al., Nucl. Phys. A **284**, 399 (1977).
[45] G. H. Herling and T. T. S. Kuo, Nucl. Phys. A **181**, 113 (1972).
[46] E. K. Warburton and B. A. Brown, Phys. Rev. C **43**, 602 (1991).
[47] Zs. Podolyák *et al.*, Phys. Lett. B **672**, 116 (2009).
[48] Zs. Podolyák *et al.*, Eur.Phys.J. A **42**, 489 (2009).
[49] N. Yoshinaga, K. Yanase, C. Watanabe, K. Higashiyama, Prog. Theor. Exp. Phys. **2021**, 063D01 (2021).
[50] M. Shamsuzzoha Basunia, Nucl. Data Sheets **121**, 561 (2014).
[51] M.J. Martin, Nucl. Data Sheets **108**, 1583 (2007).
[52] F.G. Kondev, Nucl. Data Sheets **109**, 1527 (2008).
[53] C.J. Chiara, F.G. Kondev, Nucl. Data Sheets **111**, 141 (2010).
[54] S. Zhu, F.G. Kondev, Nucl. Data Sheets **109**, 699 (2008).
[55] F.G. Kondev, S. Lalkovski Nucl. Data Sheets **108**,1471 (2007).
[56] D. Kocheva *et al.* Eur. Phys. J. A **53**, 175 (2017).
[57] E. Wilson *et al.*, Phys. Lett. B **747**, 88 (2015).
[58] Zs. Podolyák, et al., J. Phys. Conf. Ser. **580**, 012010 (2015).
[59] T.A. Berry *et al.*, Phys. Rev. C **101**, 054311 (2020).
[60] I. Hamamoto, Phys. Rep. **10**, 63 (1974).
[61] C.S. Lim, W.N. Catford, R.H. Spear, Nucl. Phys. A **522**, 635 (1991)
[62] B. A. Brown, Phys. Rev. C **58**, 220 (1998).
[63] J. A. Maruhn, P.-G. Reinhard, P. D. Stevenson and A. S. Umar, Comput. Phys. Commun. **185**, 2195 (2014).
[64] P. D. Stevenson and S. Fracasso, J. Phys. G **37**, 064030 (2010)
[65] P. D. Stevenson, M. R. Strayer, J. Rikovska Stone and W. G. Newton, Int. J. Mod. Phys. E **13**, 181 (2004).
[66] C. Ellegaard, P.D.Barnes, R.Eisenstein, E.Romberg, T.S. Bhatia, T.R.Canada, Nucl. Phys. A **206**, 83 (1973).
[67] T. Kibédi, T.W. Burrows, M.B. Trzhaskovskaya, P.M. Davidson, C.W. Nestor Jr., Nucl. Instr. and Meth. A **589**, 202 (2008).
[68] E. Caurier, M. Rejmund, H. Grawe, Phys. Rev. C **67**, 054310 (2003).